Fluid Phase Equilibria 354 (2013) 156–165

Contents lists available at SciVerse ScienceDirect

Fluid Phase Equilibria

journal homepage: www.elsevier.com/locate/fluid

A new microebulliometer for the measurement of the vapor–liquid equilibrium of ionic liquid systems

Pedro J. Carvalho[a], Imran Khan[a], António Morais[a], José F.O. Granjo[b], Nuno M.C. Oliveira[b], Luís M.N.B.F. Santos[c], João A.P. Coutinho[a,*]

[a] Departamento de Química, CICECO, Universidade de Aveiro, Campus Universitário de Santiago, 3810-193 Aveiro, Portugal
[b] Departamento de Engenharia Química, Faculdade de Ciências e Tecnologia, Universidade de Coimbra, Rua Sílvio Lima – Pólo II, 3030-790 Coimbra, Portugal
[c] Centro de Investigação em Química, Departamento de Química e Bioquímica, Faculdade de Ciências da Universidade do Porto, Rua do Campo Alegre, 687, P-4169-007 Porto, Portugal

ARTICLE INFO

Article history:
Received 17 December 2012
Received in revised form 19 April 2013
Accepted 11 June 2013
Available online 19 June 2013

Keywords:
Vapor–liquid equilibrium
Ionic liquids
Water
Ethanol
Microebulliometer
NRTL

ABSTRACT

Over the last decade ionic liquids appeared as potential entrainers for extractive distillation processes. However experimental vapor–liquid equilibrium data for ionic liquid containing systems is still scarce since most conventional equilibrium cells are not adequate for these systems. To overcome that limitation a new isobaric microebulliometer, operating at pressures ranging from 0.05 to 0.1 MPa and requiring a sample volume lower than 8 mL was developed and validated in this work.

The new apparatus was used to determine isobaric VLE data at pressures of 0.05, 0.07 and 0.1 MPa for eight binary mixtures of 1-ethyl-3-methylimidazolium chloride ([C_2mim][Cl]), 1-butyl-3-methylimidazolium chloride ([C_4mim][Cl]), 1-hexyl-3-methylimidazolium chloride ([C_6mim][Cl]), and choline chloride ([$N_{111(2OH)}$][Cl]) with water and ethanol. The experimental data here measured were correlated with the NRTL model.

1. Introduction

Distillation is still the most used separation process in the chemical industry and also one of the most energy intensive operations, for which small improvements may turn into large operational and cost advantages. One of the most challenging areas in applying distillation is the separation of azeotropic mixtures. Extractive distillation stands as one of the best approaches to deal with these systems, allowing the entrainer to be kept in the liquid phase from where it is later separated in a secondary distillation and, therefore, be reused. Organic solvents, inorganic salts and hyper-branched polymers have been investigated as entrainers [1]. Recently, ionic liquids (ILs) a novel class of solvents have attracted an increased interest as entrainers for extractive distillation [2].

Ionic liquids (ILs) are salts composed of large organic cations and organic or inorganic anions that cannot form an ordered crystal and thus remain liquid at or near room temperature. They have been reported to have good entrainer characteristics for azeotrope separation [3]. Their negligible flammability and vapor pressure, high thermal stability and solvating capacity for both polar and non-polar compounds confer them several advantages over other entrainers. Moreover, the physical and corrosion properties are more favorable, for separation processes, than those of the commonly used inorganic molten salts or high-branched polymers [3]. Arlt and co-workers [4] first proposed the use of ionic liquids as potential solvents in extractive distillation to separate water–ethanol mixtures. The authors studied imidazolium-based ILs, with chloride and tetrafluoborate anions, and concluded that these solvents are capable of breaking the water–ethanol azeotrope [4]. A recent work by Rebelo's group [3] reviews the publications on azeotrope breaking using ILs, concluding that imidazolium-based ILs with the chloride anion stands as one of the most promising choices, even over the conventional entrainer, 1,2-ethanediol [4], or even compared with the most overall effective, $CaCl_2$ [3]. Nevertheless, and despite the increasing number of publications experimental data is still scarce [5–7], to adequately design or select the optimal ionic liquid among the 106 potential ILs [8]. One major issue that limits the measurement of vapor–liquid equilibrium in systems containing ionic liquids is that the available equipments, developed for conventional solvents, require a large sample volume: Wang et al. [9] reported VLE data measured using an apparatus from Tokyo Rika Kikai Co. with a total volume of 500 cm^3 of which about 250 cm^3 is occupied by the sample; Zhao et al. [6] used a dual circulation vapor–liquid equilibrium still, with

* Corresponding author. Tel.: +351 234 401 507; fax: +351 234 370 084.
E-mail address: jcoutinho@ua.pt (J.A.P. Coutinho).

0378-3812/$ – see front matter © 2013 Elsevier B.V. All rights reserved.
http://dx.doi.org/10.1016/j.fluid.2013.06.015

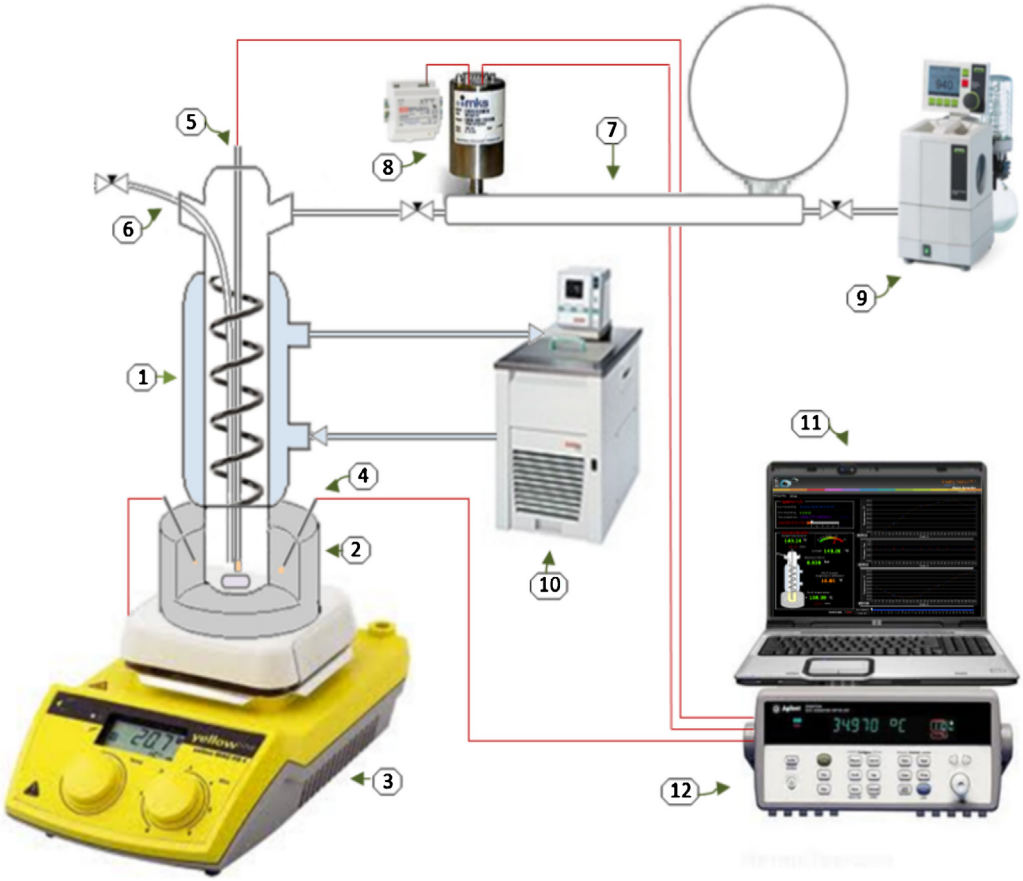

Fig. 1. Ebulliometer schematic. 1 – ebulliometer, 2 – aluminum block, 3 – heating/magnetic stirrer plate with a Pt1000 probe, 4, 5 – Pt100 probes, 6 – sampling/injection port, 7 – vacuum line, 8 – Baratron heated capacitance manometer 728A MKS with tension source, 9 – Büchi® vacuum system with a V-700 vacuum pump and V-850 controller, 10 – thermostat bath (Julabo F25 MC), 11 – computer to data acquisition, 12 – Agilent 34970A data acquisition/switch unit.

an approximate total volume of the still of 120 cm^3, requiring about 80 cm^3 of sample; Chen et al. [10] used recirculation VLE still with internal volume of about 120 cm^3 of which the liquid occupied about 100 cm^3. The VLE cell used by most researchers on this field such as Alvarez et al. [7], Andreatta et al. [11,12] and Calvar et al. [5,13,14] is a glass Fischer Labodest equilibrium still that requires a sample volume of circa 35 cm^3. Consequently, measurements of ionic liquid systems using these equipments are quite expensive and the high viscosity of the mixtures rich in ionic liquid difficult a regular boiling of the mixture.

To overcome these limitations a new isobaric ebulliometer able to operate at pressures ranging from 0.05 to 0.1 MPa, and requiring a sample volume lower than 8 cm^3 was developed, validated and used to determine vapor–liquid equilibria of eight systems of ethanol/water + chloride-based ILs.

2. Experimental

2.1. Materials

Four ILs based on the chloride anion, 1-ethyl-3-methyl imidazolium chloride ([C_2mim][Cl]), 1-butyl-3-methylimid azolium chloride ([C_4mim][Cl]), 1-hexyl-3-methylimidazolium chloride ([C_6mim][Cl]), and 2-hydroxy-*N*,*N*,*N*-trimethylamm onium chloride ([$N_{111(2OH)}$][Cl], a.k.a. choline chloride), were used in this study. The 1-alkyl-3-methylimidazolium chloride ILs were obtained from Io·li·tec with mass fraction purities higher than 98%. The 2-hydroxy-*N*,*N*,*N*-trimethylammonium chloride was obtained from Sigma–Aldrich with mass fraction purity higher than 99%. To reduce to negligible values both water and volatile compounds, high vacuum (10^{-5} mbar), stirring, and moderate temperature (303 K) for a period of at least 48 h were applied prior to the measurements. The final IL water content was determined with a Mettler Toledo DL32 Karl Fischer coulometer (using the Hydranal – Coulomat E from Riedel-de Haen as analyte), indicating a water mass fraction lower than 30×10^{-6}. The purity of each ionic liquid was further checked by ^{1}H and ^{13}C NMR.

The ethanol used was obtained from Merck with mass fraction purity higher than 99.8%. Being highly hygroscopic, the ethanol was kept under low water content through the use of molecular sieves immersed within the compound. Furthermore the ionic liquid, prior to use, was kept under low vacuum (10^{-2} mbar). The water used was double distilled and deionized. The decane and *p*-xylene was obtained from Aldrich and Acros Organics respectively, with mass fraction purity higher than 99.8%.

2.2. Experimental equipment

A new isobaric ebulliometer able to operate at pressures ranging from 0.05 up to 0.1 MPa, was designed, assembled and tested in our laboratory. The ebulliometer, schematically presented in Fig. 1, is composed by three sections: a glass sample chamber container, with a total volume of 8 mL, settled inside of an aluminum block placed on top of an heating/stirring plate; a glass condenser, surrounding the top section of the ebulliometer sample chamber, where the temperature is kept constant by means of a thermostatic bath; a liquid sampling/injection, temperature probe and pressure line connections, done by means of vacuum tide

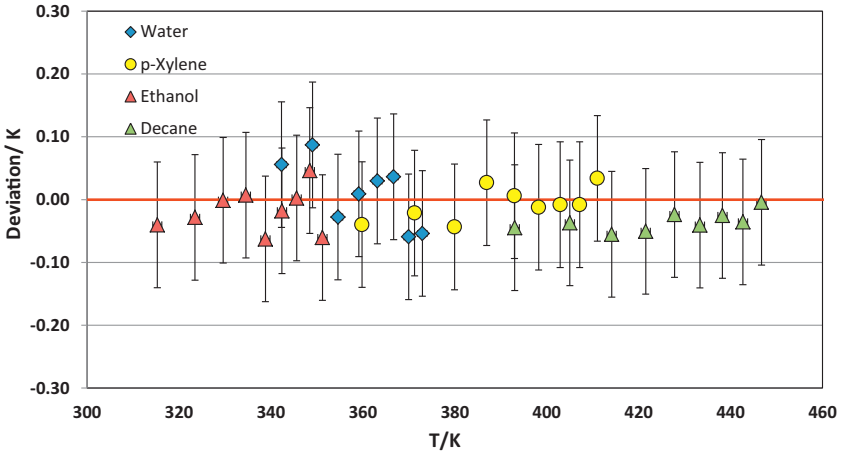

Fig. 2. Average deviations for the boiling temperatures as function of pressure. Experimental boiling temperatures calculated from NIST webbook of Chemistry [21] and DIPPR's database [22].

teflon sealed ports. Inside the ebulliometer top section a removable glass spiral increases the surface area of the reflux/condenser and the condenser, placed immediately above the sample chamber and connected to a thermostatic bath, assure a better condensation of the vapor phase generated. Some effort was done in the design of this new ebulliometer to have an optimal (low) temperature difference between the evaporation region and the condenser walls in order to establish a regular reflux with a small energy (heat) balance (low recirculation heat and mass flow). This design strategy makes possible the measurement of the equilibrium temperatures in conditions of small fractions of volatile component. The cylindrical aluminum block, with its smooth external wall and the sample chamber placed on its geometrical center, together with the small magnetic stirrer placed inside the ebulliometer sample chamber allows good homogenization of the sample concentration and temperature. The pressure is controlled and kept constant trough a vacuum line, with an internal volume of 5×10^{-3} m^3, connected to a Büchi V-700 vacuum pump and V-850 pressure monitoring and controller unit. Pressure measurements are done using a Baratron type capacitance Manometer, MKS model 728A, with temperature regulation at 100 °C to avoid solvent condensation and with an accuracy of 0.5%. The large volume of the vacuum line allows a better pressure regulation. A metallic sealed Pt100 class A temperature probe placed in the aluminum block, close to the ebulliometer cavity, is used to measures and control the temperature of the heater block. The temperature of the liquid phase inside the ebulliometer is measured by means of a fast response glass sealed Pt100 class 1/10, calibrated previously against a calibrated platinum resistance thermometer, SPRT100 (Fluke-Hart Scientific 1529 Chub-E4), traceable to the National Institute of Standards and Technology (NIST), with an uncertainty less than 2×10^{-2}.

A mixture rich in ethanol or water is introduced inside the ebulliometer sample chamber and allowed to reach equilibrium, with constant and smooth boiling. Once the equilibrium is reached, the boiling temperature is measured, the liquid phase sampled and the mixture composition determined through an Anton Paar Abbemat 500 Refractometer, with an uncertainty of 2×10^{-5} nD, using a calibration curve previously established. This procedure allows the determination of the sample composition within ±0.001 mol fraction. Subsequently, fixed amounts of IL, water or ethanol are introduced into the ebulliometer, to change the mixture composition, and the procedure is repeated. The IL is kept under moderate vacuum (10^{-2} mbar) between measurements, to assure no water absorption from atmosphere.

Since no reference data is available on the literature for these systems, and the amount of available data is quite limited, the adequacy of the apparatus to measure this type of systems is here established using the measurements of vapor–liquid equilibrium data for pure compounds (ethanol, water, *p*-xylene and decane) covering the temperature range of operation of the equipment and the binary systems [C_4mim][Cl] + H_2O, and [C_4mim][Cl] + ethanol [5], and [C_6mim][Cl] + H_2O [15].

3. VLE modeling with the NRTL model

The experimental data gathered was correlated using the NRTL model [16] to predict the non-ideal behavior of the liquid phase solution. This model is based on the local composition concept, to express the effect of the intermolecular forces (short-range) in the non-randomness of the mixtures, using only binary interaction parameters that are estimated from experimental data. For each binary molecular pair *i*–*j*, the model has three parameters – two interaction parameters Δg_{ij} and Δg_{ji} and the non-randomness parameter α_{ij} ($\alpha_{ij} = \alpha_{ji}$). The expressions for the excess Gibbs energy (g^E) and the logarithm of the activity coefficient ($\ln \gamma_i$) given by the NRTL model can be written as [17]:

$$\frac{g^E}{RT} = \sum_i^{n_c} x_i \ln \gamma_i = \sum_i^{n_c} \frac{x_i L_i}{M_i} \tag{1}$$

$$\ln \gamma_i = \frac{L_i}{M_i} + \sum_j^{n_c} \frac{x_j G_{ij}}{M_j} \left(\tau_{ij} - \frac{L_j}{M_j} \right) \tag{2}$$

$$L_i = \sum_k^{n_c} x_k \tau_{ki} G_{ki} \tag{3}$$

$$M_i = \sum_k^{n_c} x_k G_{ki} \tag{4}$$

$$G_{ij} = e^{-\alpha_{ij}\tau_{ij}} \tag{5}$$

$$\tau_{ij} = \frac{(g_{ij} - g_{ii})}{RT} = \frac{\Delta g_{ij}}{RT}, \quad i \neq j \quad \text{and} \quad \tau_{ij} = 0, \; i = j \tag{6}$$

here $i, j, k \in \{1, 2, 3\}$ represent the different molecular species in the mixture (1 – water, 2 – ethanol, 3 – IL), n_c corresponds to the number of components and x_i refers to molar fractions.

Table 1
Vapor–liquid equilibrium data for the $[C_2mim][Cl] + H_2O$ system at 0.1, 0.07 and 0.05 MPa.[a]

x_{H_2O}	T (K)	γ_{H_2O}	x_{H_2O}	T (K)	γ_{H_2O}	x_{H_2O}	T (K)	γ_{H_2O}	x_{H_2O}	T (K)	γ_{H_2O}	x_{H_2O}	T (K)	γ_{H_2O}	x_{H_2O}	T (K)	γ_{H_2O}
0.1 MPa						0.07 MPa						0.05 MPa					
0.998	373.66	0.970	0.749	400.00	0.541	0.998	364.02	0.966	0.780	383.59	0.615	0.998	355.58	0.959	0.806	371.07	0.661
0.975	374.88	0.950	0.736	401.71	0.524	0.983	364.72	0.955	0.757	387.45	0.558	0.991	355.66	0.959	0.789	373.68	0.613
0.966	375.65	0.934	0.719	404.71	0.490	0.972	365.06	0.952	0.752	388.47	0.544	0.979	356.24	0.951	0.774	375.36	0.590
0.955	376.19	0.928	0.713	406.30	0.473	0.955	366.46	0.922	0.746	389.39	0.532	0.970	356.56	0.949	0.756	378.59	0.539
0.939	377.52	0.902	0.693	409.47	0.444	0.949	366.67	0.918	0.733	391.36	0.508	0.954	357.69	0.922	0.745	379.47	0.532
0.923	378.51	0.885	0.663	414.52	0.402	0.929	368.25	0.886	0.722	393.61	0.480	0.943	358.36	0.906	0.708	385.15	0.462
0.909	379.96	0.853	0.654	416.30	0.388	0.907	370.05	0.849	0.713	394.65	0.472	0.927	359.36	0.886	0.698	386.47	0.449
0.898	381.12	0.831	0.645	418.65	0.369	0.902	370.30	0.845	0.689	398.79	0.429	0.910	360.94	0.855	0.679	389.51	0.418
0.886	382.25	0.811	0.636	419.93	0.361	0.888	371.42	0.825	0.659	403.11	0.393	0.903	361.33	0.849	0.670	391.27	0.400
0.868	384.12	0.778	0.625	422.01	0.348	0.877	372.64	0.800	0.651	405.98	0.366	0.892	362.22	0.828	0.653	393.93	0.377
0.843	387.10	0.725	0.617	425.00	0.324	0.859	374.55	0.763	0.636	409.01	0.343	0.892	362.22	0.828	0.641	395.61	0.365
0.824	389.34	0.689	0.603	426.90	0.315	0.840	376.36	0.732	0.618	413.90	0.307	0.879	363.41	0.801	0.636	397.54	0.346
0.813	390.14	0.681	0.592	430.32	0.294	0.832	377.78	0.703	0.598	417.70	0.284	0.866	364.44	0.783	0.618	402.00	0.310
0.798	392.58	0.641	0.582	431.99	0.286	0.822	378.36	0.698	0.592	418.77	0.279	0.859	365.26	0.767	0.593	407.18	0.277
0.777	394.56	0.618	0.568	435.03	0.271	0.812	379.90	0.670	0.578	421.93	0.263	0.843	367.61	0.713	0.580	409.30	0.266
0.763	396.80	0.587				0.793	382.37	0.631				0.826	369.65	0.675			

[a] Standard uncertainties x, T and γ are 0.001, 0.02 K and 0.001, respectively.

Table 2
Vapor–liquid equilibrium data for the $[C_4mim][Cl] + H_2O$ system at 0.1, 0.07 and 0.05 MPa.[a]

x_{H_2O}	T (K)	γ_{H_2O}	x_{H_2O}	T (K)	γ_{H_2O}	x_{H_2O}	T (K)	γ_{H_2O}	x_{H_2O}	T (K)	γ_{H_2O}	x_{H_2O}	T (K)	γ_{H_2O}	x_{H_2O}	T (K)	γ_{H_2O}
0.1 MPa						0.07 MPa						0.05 MPa					
0.988	372.66	1.014	0.762	395.74	0.608	0.985	363.49	0.998	0.766	384.83	0.601	0.988	354.92	0.993	0.769	373.89	0.626
0.976	373.55	0.995	0.753	397.15	0.589	0.976	364.38	0.975	0.757	386.57	0.574	0.976	355.92	0.965	0.751	376.21	0.589
0.974	374.48	0.965	0.745	397.55	0.588	0.969	364.72	0.969	0.755	386.33	0.581	0.970	356.11	0.965	0.751	376.74	0.578
0.970	374.26	0.975	0.729	400.03	0.557	0.969	364.86	0.964	0.730	389.14	0.549	0.969	356.29	0.959	0.730	378.89	0.553
0.964	374.67	0.968	0.706	404.19	0.507	0.966	365.21	0.954	0.705	393.19	0.499	0.966	356.50	0.955	0.705	382.70	0.503
0.945	374.76	0.983	0.681	408.99	0.457	0.947	365.91	0.949	0.688	396.71	0.458	0.945	357.17	0.949	0.691	386.37	0.454
0.921	378.05	0.899	0.666	411.09	0.441	0.922	368.28	0.892	0.649	402.78	0.404	0.923	359.27	0.893	0.684	387.27	0.445
0.901	379.17	0.885	0.664	412.40	0.425	0.900	369.76	0.866	0.646	403.13	0.401	0.901	361.06	0.856	0.668	388.50	0.437
0.879	380.97	0.853	0.647	415.09	0.405	0.875	371.45	0.838	0.626	405.83	0.382	0.880	362.41	0.834	0.656	391.83	0.400
0.866	382.49	0.822	0.628	418.62	0.378	0.863	372.86	0.808	0.620	407.62	0.366	0.867	363.72	0.804	0.651	391.99	0.401
0.842	385.00	0.777	0.625	420.09	0.365	0.841	375.23	0.762	0.605	410.88	0.341	0.844	365.28	0.778	0.635	393.77	0.389
0.822	387.31	0.737	0.600	424.54	0.337	0.824	377.32	0.723	0.580	414.97	0.317	0.824	367.83	0.725	0.631	394.72	0.380
0.789	391.18	0.678	0.585	429.69	0.302	0.801	380.38	0.669				0.802	370.39	0.679	0.609	399.53	0.339
0.779	394.25	0.623		430.10	0.301	0.778	382.72	0.635				0.777	373.30	0.632	0.581	405.02	0.301

[a] Standard uncertainties x, T and γ are 0.001, 0.02 K and 0.001, respectively.

Table 3
Vapor–liquid equilibrium data for the $[C_6mim][Cl] + H_2O$ system at 0.1, 0.07 and 0.05 MPa.[a]

x_{H_2O}	T (K)	γ_{H_2O}	x_{H_2O}	T (K)	γ_{H_2O}	x_{H_2O}	T (K)	γ_{H_2O}	x_{H_2O}	T (K)	γ_{H_2O}	x_{H_2O}	T (K)	γ_{H_2O}	x_{H_2O}	T (K)	γ_{H_2O}
0.1 MPa						0.07 MPa						0.05 MPa					
0.996	373.13	0.988	0.853	383.08	0.818	0.996	363.46	0.989	0.853	372.29	0.833	0.996	354.64	0.994	0.853	362.87	0.842
0.994	373.39	0.983	0.840	384.20	0.800	0.993	363.56	0.986	0.840	373.49	0.810	0.994	354.70	0.994	0.840	363.37	0.839
0.991	373.66	0.978	0.836	384.59	0.794	0.991	363.74	0.983	0.829	374.67	0.788	0.991	354.83	0.992	0.832	364.28	0.818
0.984	373.79	0.977	0.832	385.09	0.784	0.984	363.90	0.983	0.821	375.61	0.769	0.984	355.02	0.991	0.830	364.89	0.802
0.980	374.03	0.973	0.820	386.27	0.765	0.980	364.14	0.978	0.820	375.70	0.768	0.982	355.19	0.986	0.827	365.21	0.795
0.976	374.33	0.967	0.813	387.08	0.752	0.975	364.45	0.971	0.819	375.83	0.765	0.975	355.42	0.984	0.806	366.01	0.792
0.965	374.57	0.969	0.808	388.02	0.734	0.966	364.86	0.966	0.808	376.32	0.762	0.966	356.03	0.970	0.806	366.09	0.790
0.954	375.10	0.963	0.796	389.15	0.718	0.956	365.37	0.957	0.800	377.54	0.738	0.956	356.69	0.955	0.800	366.60	0.781
0.945	375.57	0.956	0.787	390.07	0.705	0.949	366.01	0.943	0.786	378.83	0.718	0.950	357.06	0.947	0.786	368.16	0.750
0.933	376.13	0.949	0.776	391.17	0.690	0.937	366.49	0.938	0.778	379.36	0.712	0.936	357.43	0.947	0.781	369.03	0.731
0.918	377.09	0.933	0.767	392.23	0.675	0.920	367.27	0.927	0.775	380.34	0.692	0.920	357.96	0.944	0.774	369.71	0.720
0.912	377.80	0.917	0.758	393.39	0.659	0.912	367.94	0.912	0.761	381.53	0.677	0.912	358.91	0.918	0.761	370.34	0.716
0.901	378.60	0.902	0.744	394.83	0.641	0.902	368.70	0.898	0.747	382.80	0.660	0.903	359.94	0.890	0.753	371.27	0.699
0.887	379.60	0.885	0.718	397.29	0.615	0.888	369.79	0.875	0.725	384.70	0.639	0.889	360.40	0.888	0.721	374.92	0.641
0.879	380.37	0.870	0.694	400.21	0.582	0.880	370.33	0.866	0.699	386.81	0.617	0.881	360.93	0.878	0.702	376.29	0.627
0.871	381.25	0.851	0.668	403.25	0.552	0.873	370.95	0.854	0.671	391.39	0.555	0.875	361.50	0.865	0.670	381.29	0.553
0.864	381.96	0.838	0.649	405.30	0.534	0.864	371.80	0.837	0.655	393.61	0.530	0.864	361.83	0.865	0.655	383.26	0.530

[a] Standard uncertainties x, T and γ are 0.001, 0.02 K and 0.001, respectively.

Table 4
Vapor–liquid equilibrium data for the $[N_{111(2OH)}][Cl] + H_2O$ system at 0.1, 0.07 and 0.05 MPa.[a]

x_{H_2O}	T (K)	γ_{H_2O}	x_{H_2O}	T (K)	γ_{H_2O}	x_{H_2O}	T (K)	γ_{H_2O}	x_{H_2O}	T (K)	γ_{H_2O}	x_{H_2O}	T (K)	γ_{H_2O}	x_{H_2O}	T (K)	γ_{H_2O}
0.1 MPa						0.07 MPa						0.05 MPa					
0.985	372.46	1.021	0.859	381.60	0.854	0.985	363.70	0.991	0.859	372.24	0.829	0.985	355.11	0.984	0.860	363.24	0.824
0.985	371.97	1.043	0.806	386.80	0.766	0.982	363.47	1.001	0.809	376.75	0.751	0.982	355.15	0.990	0.810	367.70	0.740
0.979	372.93	1.013	0.754	392.77	0.675	0.979	363.69	0.997	0.754	382.62	0.658	0.980	355.93	0.960	0.761	372.65	0.659
0.971	373.12	1.014	0.705	398.97	0.595	0.972	364.03	0.992	0.705	388.36	0.582	0.972	355.71	0.978	0.704	378.69	0.577
0.955	374.00	0.999	0.670	402.54	0.562	0.959	364.72	0.978	0.670	392.82	0.531	0.959	356.36	0.966	0.671	382.75	0.527
0.941	375.08	0.978	0.635	407.78	0.508	0.944	365.71	0.957	0.632	398.47	0.472	0.943	357.19	0.948	0.629	388.91	0.458
0.933	376.35	0.942	0.618	410.03	0.490	0.933	366.16	0.954	0.619	399.90	0.462	0.936	357.67	0.940	0.623	389.14	0.460
0.923	376.33	0.953	0.614	411.12	0.477	0.924	366.91	0.935	0.612	400.27	0.462	0.924	358.26	0.929	0.619	389.79	0.453
0.900	378.19	0.917				0.900	368.71	0.899				0.900	359.88	0.895			

[a] Standard uncertainties x, T and γ are 0.001, 0.02 K and 0.001, respectively.

Although the NRTL model was not developed to describe the behavior of mixtures containing electrolyte species, it has been applied successfully in systems with ionic liquid solutions [5,18,19]. This can be explained by the fact that in ILs the ion charge is usually disperse and the long-range electrostatic forces are weak compared with the short-range intermolecular forces (so that they can be neglected). Therefore, in the present work the liquid solutions were modeled as mixtures of non-dissociated components.

Different approaches have been considered for the parameter estimation problem with the NRTL model, to obtain the best set of parameters that describe the VLE data in systems containing ionic liquids. In the present work, this task was formulated as the solution of a nonlinear programming problem (NLP), using the weighted norm of the differences between the solvent (water or ethanol) experimental mole fractions and the values predicted by the model as the objective function:

$$\min_z \varphi = \sum_l^{nt} \omega_l e_l(\Delta g_{ij})^2 \tag{7}$$

In this equation $e_l(\Delta g_{ij}) = x_l^{exp} - x_l^{mod}(\Delta g_{ij})$, where the superscripts exp and mod correspond to the solvent experimental and

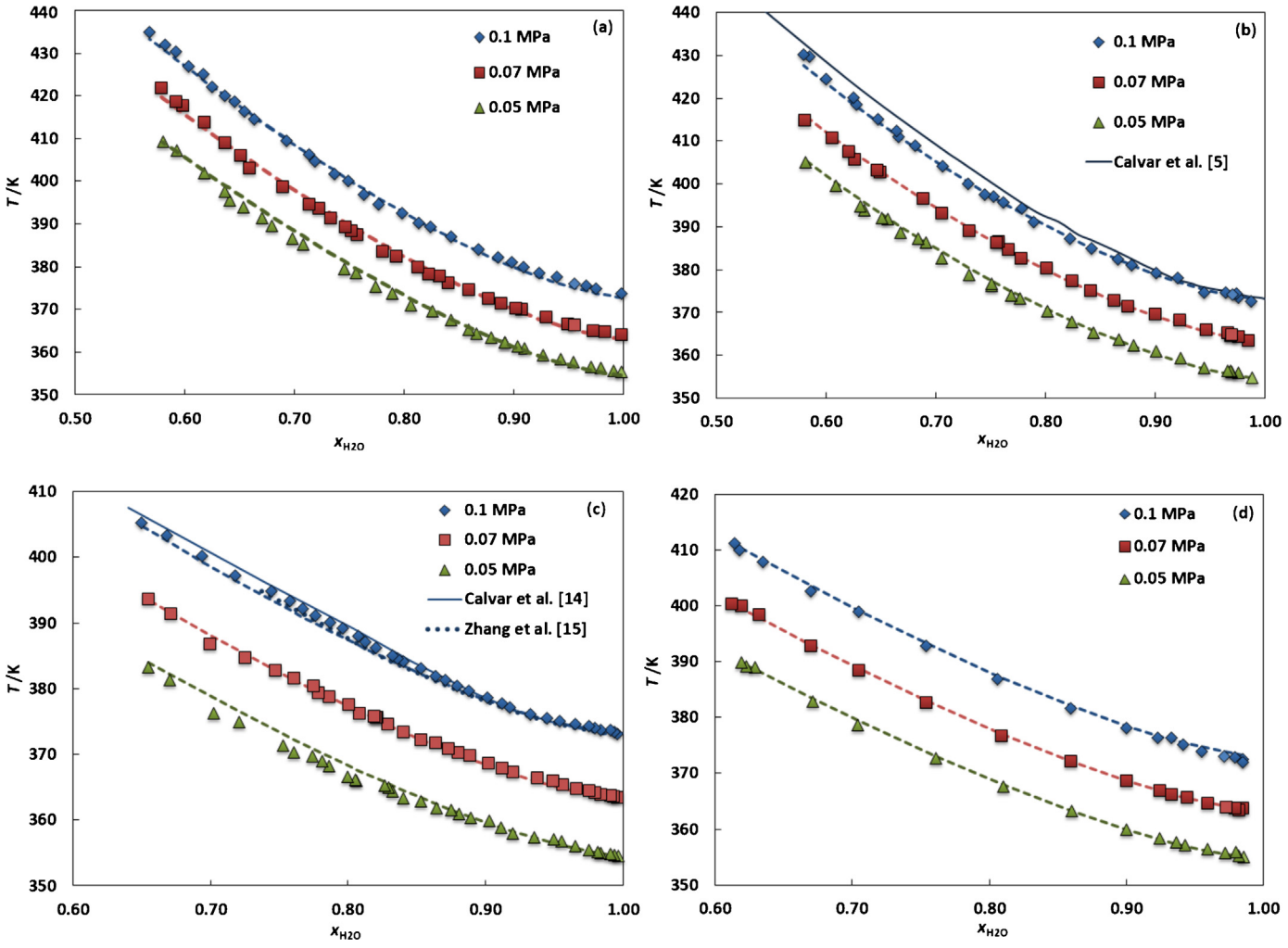

Fig. 3. Temperature–composition diagram of (a) $[C_2mim][Cl]$ + water, (b) $[C_4mim][Cl]$ + water, (c) $[C_6mim][Cl]$ + water and (d) $[N_{111(2OH)}][Cl]$+ water at 0.1, 0.07 and 0.05 MPa. The dashed lines represent the correlation of the data using the NRTL model.

Table 5
Vapor–liquid equilibrium data for the [C_2mim][Cl] + Ethanol system at 0.1, 0.07 and 0.05 MPa.[a]

x_{EtOH}	T (K)	γ_{EtOH}	x_{EtOH}	T (K)	γ_{EtOH}	x_{EtOH}	T (K)	γ_{EtOH}	x_{EtOH}	T (K)	γ_{EtOH}	x_{EtOH}	T (K)	γ_{EtOH}	x_{EtOH}	T (K)	γ_{EtOH}
0.1 MPa						0.07 MPa						0.05 MPa					
0.997	351.10	1.002	0.759	369.56	0.662	0.997	342.66	0.986	0.700	361.14	0.678	0.995	334.80	0.989	0.707	351.22	0.703
0.979	351.70	0.996	0.756	369.89	0.659	0.992	342.69	0.990	0.681	361.84	0.680	0.974	335.12	1.000	0.674	353.25	0.682
0.966	352.25	0.989	0.739	371.34	0.640	0.959	343.31	0.998	0.669	365.37	0.609	0.959	335.53	0.996	0.666	356.30	0.613
0.950	353.07	0.974	0.720	373.03	0.619	0.939	344.05	0.987	0.640	366.33	0.614	0.939	336.07	0.989	0.643	357.71	0.601
0.936	353.64	0.967	0.712	375.18	0.583	0.922	344.67	0.980	0.613	369.04	0.584	0.922	336.81	0.979	0.626	360.10	0.565
0.915	354.63	0.952	0.680	376.96	0.575	0.899	345.61	0.966	0.594	371.72	0.550	0.899	337.33	0.982	0.611	360.60	0.569
0.891	356.24	0.918	0.654	378.99	0.559	0.872	347.14	0.936	0.560	372.53	0.567	0.872	339.07	0.940	0.604	360.13	0.585
0.871	357.98	0.879	0.651	381.37	0.520	0.846	348.66	0.908	0.538	373.84	0.564	0.850	340.38	0.910	0.561	363.28	0.560
0.862	358.80	0.862	0.610	385.17	0.491	0.810	350.92	0.867	0.529	375.32	0.546	0.843	340.33	0.920	0.553	365.46	0.526
0.836	361.07	0.817	0.610	383.87	0.511	0.807	351.30	0.859	0.517	375.97	0.547	0.811	342.63	0.869	0.533	365.88	0.538
0.834	360.96	0.823	0.578	388.38	0.469	0.786	353.80	0.798	0.490	378.51	0.529	0.783	345.13	0.812	0.523	368.26	0.503
0.813	363.21	0.777	0.564	389.89	0.458	0.763	355.88	0.760	0.468	381.44	0.504	0.763	346.28	0.794	0.512	368.83	0.503
0.798	364.46	0.757	0.537	392.85	0.440	0.750	357.97	0.714				0.753	346.88	0.785	0.478	371.58	0.491
0.795	365.49	0.731	0.532	392.42	0.450	0.718	358.33	0.736				0.753	346.88	0.785			
0.784	366.90	0.706				0.706	360.00	0.703				0.728	350.03	0.716			

[a] Standard uncertainties x, T and γ are 0.001, 0.02 K and 0.001, respectively.

Table 6
Vapor–liquid equilibrium data for the [C_4mim][Cl] + ethanol system at 0.1, 0.07 and 0.05 MPa.[a]

x_{EtOH}	T (K)	γ_{EtOH}	x_{EtOH}	T (K)	γ_{EtOH}	x_{EtOH}	T (K)	γ_{EtOH}	x_{EtOH}	T (K)	γ_{EtOH}	x_{EtOH}	T (K)	γ_{EtOH}	x_{EtOH}	T (K)	γ_{EtOH}
0.1 MPa						0.07 MPa						0.05 MPa					
1.000	351.07	0.999	0.749	368.11	0.706	1.000	342.76	0.980	0.780	357.23	0.707	1.000	335.03	0.972	0.736	354.35	0.598
0.983	351.42	1.003	0.734	371.50	0.640	0.983	342.87	0.991	0.776	356.19	0.739	0.983	335.25	0.984	0.711	356.97	0.560
0.977	351.51	1.005	0.703	375.06	0.592	0.977	342.83	1.000	0.768	358.07	0.695	0.971	334.77	1.016	0.710	357.22	0.555
0.951	352.63	0.986	0.681	378.76	0.541	0.963	343.25	0.997	0.734	362.81	0.610	0.959	335.55	0.997	0.683	359.18	0.536
0.944	352.98	0.981	0.673	379.12	0.540	0.955	343.59	0.992	0.714	365.59	0.568	0.931	336.70	0.976	0.673	361.50	0.499
0.922	353.72	0.976	0.655	380.76	0.526	0.943	343.97	0.987	0.685	368.88	0.527	0.925	337.33	0.954	0.649	363.33	0.484
0.917	353.45	0.992	0.647	382.60	0.502	0.925	345.17	0.959	0.669	369.74	0.522	0.887	339.37	0.910	0.642	364.63	0.468
0.886	356.11	0.928	0.625	385.78	0.469	0.897	346.41	0.940	0.654	372.06	0.494	0.886	339.20	0.923	0.617	367.44	0.442
0.855	358.54	0.876	0.613	387.01	0.460	0.887	347.36	0.915	0.645	372.93	0.486	0.857	341.51	0.864	0.592	370.22	0.416
0.848	358.64	0.881	0.601	390.06	0.427	0.861	348.76	0.891	0.624	376.51	0.445	0.849	341.57	0.869	0.579	372.04	0.398
0.829	361.14	0.821	0.571	395.14	0.385	0.856	349.48	0.871	0.596	381.44	0.396	0.826	343.80	0.812	0.557	374.57	0.380
0.818	361.25	0.827	0.543	399.20	0.360	0.848	349.56	0.876	0.575	384.38	0.373	0.819	343.56	0.828	0.532	378.17	0.353
0.796	364.39	0.758	0.542	399.37	0.359	0.825	352.12	0.814	0.544	389.12	0.339	0.797	346.44	0.758	0.513	381.62	0.328
0.781	365.12	0.753	0.522	402.03	0.345	0.819	352.01	0.824	0.519	391.89	0.327	0.779	349.33	0.689	0.482	385.12	0.312
0.767	367.83	0.696	0.500	405.89	0.323	0.797	354.89	0.756	0.497	394.68	0.314	0.768	351.05	0.652	0.459	388.33	0.296

[a] Standard uncertainties x, T and γ are 0.001, 0.02 K and 0.001, respectively.

calculated mole fraction values, respectively. The summation in this equation is taken over all VLE data points (l) of each binary molecular pair (water–IL or ethanol–IL), and ω_l is a weight factor associated with each error term. The objective function φ was minimized by simultaneous determination of all quantities (parameters and model predictions, collectively denoted by z), subjected to constraints of VLE (Eq. (7)), the NRTL activity coefficient model (Eqs. (1)–(6)), sum of molar fraction restrictions, and magnitude bounds for the model parameters Δg_{ij}. The α_{ij} parameters in the model were considered constant, with $\alpha_{13} = 0.2$ and $\alpha_{23} = 0.3$, as suggested by Chapeaux et al. [20]. The weights ω_l were considered to be unitary for all data points available.

4. Results and discussion

4.1. Experimental results

In the absence of reference data for VLE of ionic liquid containing systems the new microebulliometer developed on this work was validated on the measurement of boiling temperatures of the

Table 7
Vapor–liquid equilibrium data for the [C_6mim][Cl] + Ethanol system at 0.1, 0.07 and 0.05 MPa.[a]

x_{EtOH}	T (K)	γ_{EtOH}	x_{EtOH}	T (K)	γ_{EtOH}	x_{EtOH}	T (K)	γ_{EtOH}	x_{EtOH}	T (K)	γ_{EtOH}	x_{EtOH}	T (K)	γ_{EtOH}	x_{EtOH}	T (K)	γ_{EtOH}
0.1 MPa						0.07 MPa						0.05 MPa					
0.991	351.94	0.974	0.750	370.60	0.647	0.993	343.07	0.974	0.752	360.47	0.649	0.992	335.15	0.980	0.751	351.72	0.648
0.974	352.21	0.981	0.730	373.20	0.608	0.970	343.26	0.989	0.734	362.56	0.615	0.971	335.30	0.991	0.733	354.48	0.596
0.962	352.57	0.978	0.707	376.26	0.566	0.962	343.63	0.981	0.709	365.90	0.566	0.962	335.76	0.981	0.708	357.44	0.551
0.949	352.97	0.976	0.682	379.50	0.527	0.950	344.05	0.977	0.681	369.39	0.521	0.949	336.27	0.972	0.678	359.90	0.525
0.932	353.90	0.959	0.658	383.21	0.484	0.933	344.87	0.962	0.656	372.70	0.481	0.932	336.96	0.960	0.657	363.86	0.468
0.913	354.93	0.941	0.625	388.96	0.425	0.913	345.75	0.949	0.623	377.17	0.435	0.911	337.75	0.953	0.625	367.07	0.440
0.884	356.83	0.905	0.605	392.29	0.396	0.883	347.68	0.907	0.605	381.50	0.389	0.883	339.57	0.906	0.600	371.50	0.392
0.858	358.79	0.865	0.588	394.60	0.380	0.866	348.82	0.882	0.578	385.14	0.363	0.866	340.62	0.885	0.574	375.08	0.362
0.848	359.84	0.842	0.576	396.89	0.363	0.848	349.98	0.860	0.560	389.18	0.330	0.850	341.68	0.863	0.548	379.08	0.333
0.822	362.09	0.800	0.550	401.81	0.329	0.823	352.13	0.815	0.551	391.16	0.316	0.823	343.36	0.830	0.520	381.16	0.328
0.808	364.19	0.753	0.521	406.86	0.302	0.808	354.04	0.770	0.521	395.70	0.291	0.808	345.20	0.784	0.502	385.72	0.292
0.788	366.36	0.714	0.504	411.86	0.272	0.788	356.13	0.729	0.504	399.58	0.268	0.787	347.26	0.740	0.463	389.46	0.283
0.767	368.68	0.676				0.769	358.19	0.691				0.769	349.20	0.700			

[a] Standard uncertainties x, T and γ are 0.001, 0.02 K and 0.001, respectively.

Table 8
Vapor–liquid equilibrium data for the $[N_{111(2OH)}][Cl]$ + ethanol system at 0.1, 0.07 and 0.05 MPa.[a]

x_{EtOH}	T (K)	γ_{EtOH}	x_{EtOH}	T (K)	γ_{EtOH}	x_{EtOH}	T (K)	γ_{EtOH}	x_{EtOH}	T (K)	γ_{EtOH}	x_{EtOH}	T (K)	γ_{EtOH}	x_{EtOH}	T (K)	γ_{EtOH}
0.1 MPa						0.07 MPa						0.05 MPa					
0.996	351.06	0.999	0.947	352.12	1.009	0.995	342.62	0.989	0.949	343.29	1.011	0.995	334.99	0.982	0.952	335.54	1.002
0.995	351.48	0.984	0.947	352.13	1.007	0.989	342.53	1.000	0.947	343.51	1.002	0.989	334.81	0.997	0.949	335.55	1.007
0.990	351.21	1.000	0.944	352.69	0.992	0.981	342.66	1.002	0.947	343.37	1.010	0.981	334.88	1.001	0.944	335.80	1.002
0.983	351.20	1.009	0.943	352.36	1.006	0.972	343.02	0.998	0.944	343.48	1.006	0.972	335.22	0.998	0.943	335.78	1.002
0.972	351.88	0.991	0.940	352.86	0.990	0.966	343.05	1.002	0.942	343.56	1.005	0.965	335.31	0.999	0.939	335.84	1.003
0.967	351.62	1.008	0.935	352.89	0.994	0.963	343.19	1.000	0.939	343.87	0.997	0.963	335.52	0.994	0.935	335.86	1.006
0.963	351.71	1.010	0.933	352.90	0.995	0.962	343.17	1.002	0.935	343.90	1.001	0.962	335.39	0.996	0.934	335.87	1.008
0.956	351.99	1.003	0.931	352.88	0.999	0.956	343.37	0.998	0.931	343.87	1.007	0.956	335.59	0.996	0.931	335.89	1.012
0.951	352.17	1.006	0.926	353.06	0.994	0.953	343.27	1.007	0.925	344.03	1.005	0.952	335.61	1.001	0.924	336.00	1.010
0.950	352.16	1.008				0.952	343.56	0.996				0.952	335.54	1.002			

[a] Standard uncertainties x, T and γ are 0.001, 0.02 K and 0.001, respectively.

pure compounds ethanol, water, *p*-xylene and decane, chosen to cover the temperature range of operation of the ebulliometer comprised between 310 and 450 K. At each pressure at least 5 boiling temperatures were measured and the average value and the corresponding standard deviation are presented. The deviations against the boiling temperatures estimated from the vapor pressure correlations reported at NIST Webbook of Chemistry [21] and the DIPPR database [22] are shown in Fig. 2. An uncertainty on the boiling temperatures of ±0.1 K was obtained.

Experimental isobaric VLE data of the binary systems $[C_2mim][Cl] + H_2O$, $[C_4mim][Cl] + H_2O$, $[C_6mim][Cl] + H_2O$ and $[N_{111(2OH)}][Cl] + H_2O$ were measured at 0.1, 0.07 and 0.05 MPa, and are reported in Tables 1–4 and depicted in Fig. 3. The 0.1 MPa isobaric VLE data of $[C_4mim][Cl] + H_2O$ and $[C_6mim][Cl] + H_2O$ are here compared with those of Calvar et al. [5], and those of $[C_6mim][Cl] + H_2O$ are also compared with the data by Zhang et al. [15]. The boiling temperatures measured in this work show a good agreement with the literature data for the more diluted solutions, with percentage absolute average deviations (%AAD) of 0.28% and 0.14% for the Calvar et al. [5] $[C_4mim][Cl] + H_2O$ and $[C_6mim][Cl] + H_2O$ systems, respectively, and 0.16% for the Zhang et al. [15] $[C_6mim][Cl] + H_2O$ system. For systems with higher concentrations of ionic liquid and higher temperatures our data for the $[C_6mim][Cl] + H_2O$ system are in good agreement with

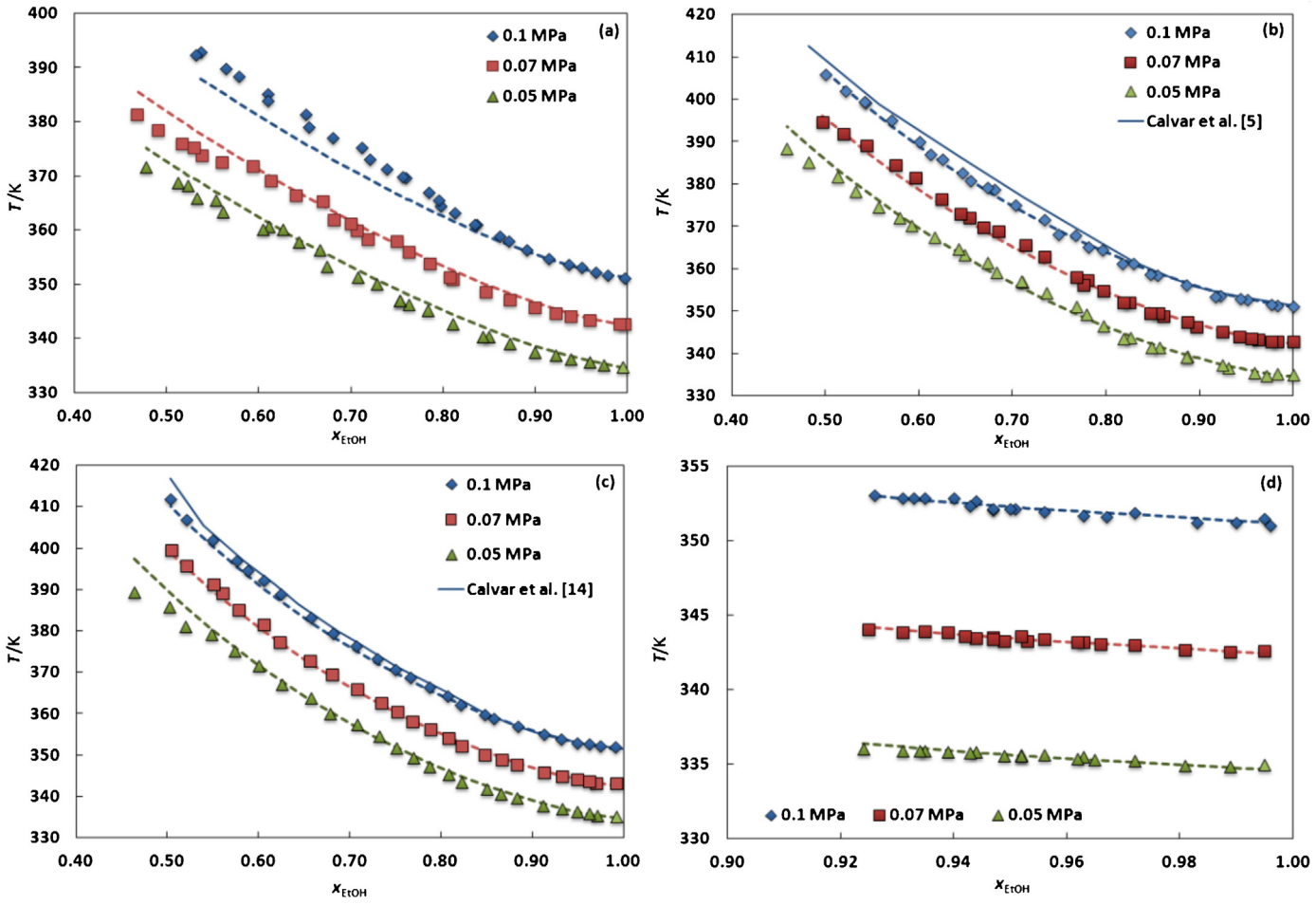

Fig. 4. Temperature–composition diagram of (a) $[C_2mim][Cl]$ + ethanol, (b) $[C_4mim][Cl]$ + ethanol, (c) $[C_6mim][Cl]$ + ethanol, and (d) $[N_{111(2OH)}][Cl]$ + ethanol at 0.1, 0.07 and 0.05 MPa. The dashed lines represent the correlation of the data using the NRTL model.

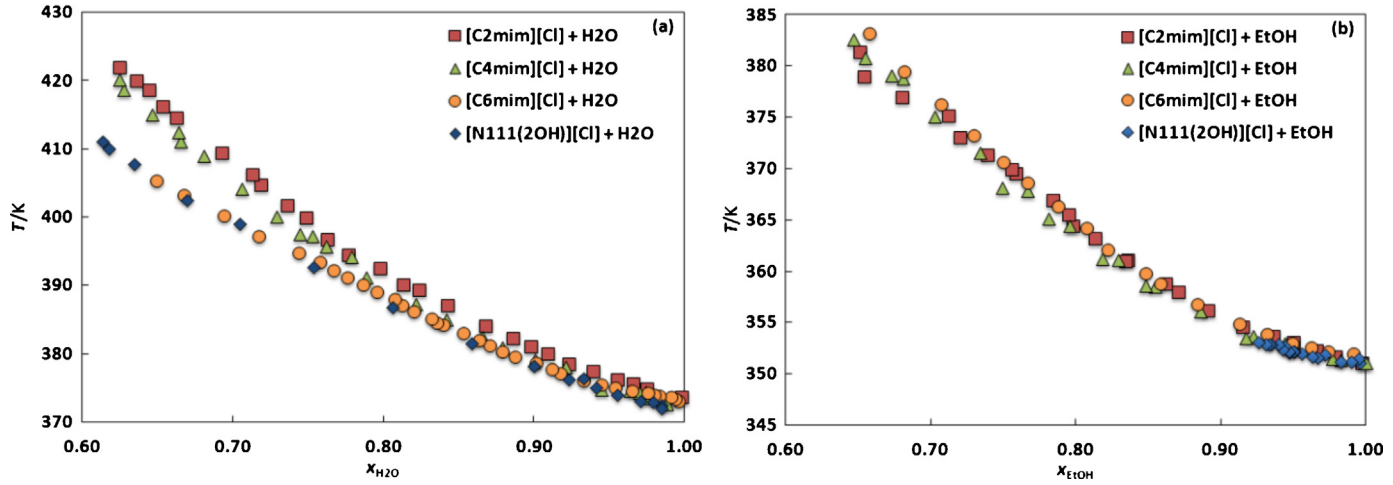

Fig. 5. Temperature–composition diagram of (a) water + [C_2mim][Cl], [C_4mim][Cl], [C_6mim][Cl]and [$N_{111(2OH)}$][Cl], (b) ethanol + [C_2mim][Cl], [C_4mim][Cl], [C_6mim][Cl] and [$N_{111(2OH)}$][Cl] at 0.1 MPa.

the data by Zhang et al. [15] but some deviations are observed between these two sets of data and the data by Calvar et al. [5] that for both this system and the [C_4mim][Cl] + H_2O system systematically presents higher boiling temperatures for the higher IL concentrations. These may be due to overheating of the samples due to the difficulty to achieve a regular boiling on a large volume apparatus for these concentrated and viscous solutions.

Experimental isobaric VLE data, at 0.1, 0.07 and 0.05 MPa, were also measured for the systems [C_2mim][Cl] + ethanol, [C_4mim][Cl] + ethanol, [C_6mim][Cl] + ethanol and [$N_{111(2OH)}$][Cl] + Ethanol in the region of complete miscibility. As reported in Tables 5–8 and depicted in Fig. 4, the mixture boiling temperatures were measured for IL molar fractions up to 0.35. For the choline chloride its limited miscibility in ethanol restricted the VLE measurements to IL molar fractions below 0.07. Albeit a slight deviation is still observed at high IL concentrations a good agreement between the data reported in this work and those by Calvar et al. [5] for the system [C_6mim][Cl] + ethanol is observed, with a %AAD of 0.21%. The system [C4mim][Cl] + ethanol presents a %AAD of 0.44%.

An evaluation of the influence of the cation influence on the VLE of the studied systems, presented in Fig. 5, shows some impact of the cation type and alkyl chain length upon the water systems with lower boiling points occurring with increasing alkyl chain length, that reflects the poorer solvation of these cations with longer chains. Curiously, unlike what is observed for the aqueous systems, the ethanol + ILs systems present almost no influence of the cation that could be related with the no differentiation of the solvation of the alkyl chain by the ethanol.

To analyze and compare the interactions water-IL with ethanol-IL and evaluate their impact upon the VLE behavior the activity coefficients of the solvents, water and ethanol, were estimated using the following phase equilibrium equation

$$\gamma^i = \frac{y_i \varphi_i p}{x_i \varphi_i^{\sigma} p_i^{\sigma}} \tag{8}$$

where p and p^{σ} are the pressure of the system and the saturation vapor pressure of the pure component i at the system temperature, x_i and y_i represent the mole fractions of component i in the liquid and vapor phases, ϕ_i is the fugacity coefficient of component i in the vapor phase, while φ_i^{σ} is the fugacity coefficient of component i in its saturated state. The ϕ_i and φ_i^{σ} are very close to unit for the systems studied at these low pressures and high temperatures. Since the ionic liquid is non-volatile the vapor phase is only composed of solvent and therefore y_i is equal to one. Thus, the solvent activity coefficient in solution can be simplified as

$$\gamma^i = \frac{p}{x_i p_i^{\sigma}} \tag{9}$$

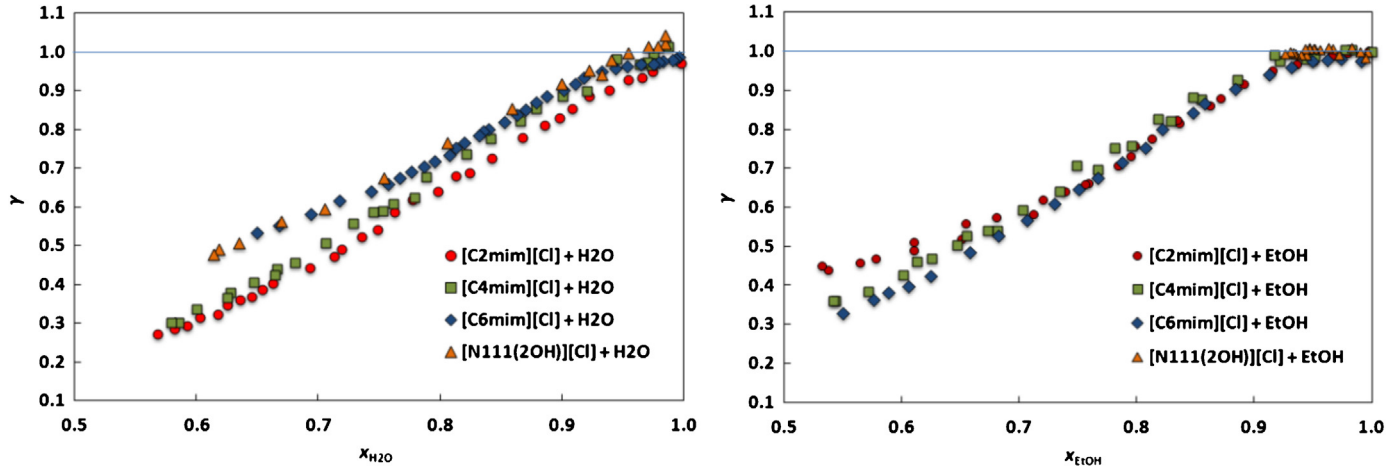

Fig. 6. Activity coefficients as function of water/ethanol mole fractions of the experimental VLE data at 0.1 MPa.

where subscript *i* refers to the solvent, water or ethanol. The water and ethanol pure component saturation vapor pressures, p^{σ}, were calculated using correlations obtained from DIPPR's database [22].

The activity coefficients estimated for the studied systems are presented in Fig. 6. It can be observed that all the systems present negative deviations to ideality ($\gamma < 1$), suggesting that the interactions between the ionic liquids and the solvents are favorable. The water + IL systems present activity coefficients that are lower than those for ethanol + IL mixtures denoting, thus, more favorable interactions between the water and the IL than with the ethanol. An almost linear decrease on the activity coefficient of water and ethanol with the increase of the ILs mole fraction is observed between 0.9 and 0.7 mole fraction, in agreement with an increase of the concentration of the ionic liquids and the solvent (water and ethanol) that is an indication of a strong specific interaction of 1:1 between the IL and the solvent. It is interesting to suggest that the decrease of the activity coefficient is pointing out to maximum activity for a mole fraction around 0.33 (2 ILs:1 H_20/ethanol), indicating the right molecular ratio between the IL and the (H-bond) solvent.

As expected from the boiling temperatures presented in Fig. 4, and confirmed by the activity coefficients of Fig. 6, the choline chloride, albeit presenting favorable interactions with the water, present interactions clearly less strong than those of imidazolium based ionic liquids. This, along with the very high melting point of this compound and its poor solubility in ethanol suggests that choline chloride is the worst option, among the ionic liquids studied on this work, for breaking the ethanol–water azeotrope.

The strong negative deviations to the ideality, with activity coefficients for equimolar mixtures below 0.5, are not particular for the systems here reported but can be found in a large number of isobaric VLE systems containing ionic liquids previously reported in the literature [3,5,7,14].

An evaluation of the influence of the pressure on the VLE of the studied systems, presented in Figs. 3 and 4, shows that the pressure drop leads to lower boiling points, as would be expected from Eq. (9). Although the boiling points decrease with the pressure, the same behavior is not observed for the activity coefficients. As depicted in Fig. 7, the differences between the activity coefficients at the various pressures are quite small, often within the experimental uncertainty, what is in good agreement with the excess volumes observed for the systems studied.

Relatively to the numerical solution of the NLP problem in Eq. (2), which often leads to multiple local optimal solutions, this was implemented in GAMS [21], and tackled using the CONOPT [23] and OQNLP [24] solvers. The computer requirements for the parameter estimation task were of the order of one second of CPU for CONOPT and were allowed a maximum of 60 CPU minutes for the runs with the OQNLP solver, on an Intel Xeon 5570 Linux workstation. By taking advantage of the multistart feature of the OQNLP solver, an extensive search for alternative solutions was performed within the computation time established. The values

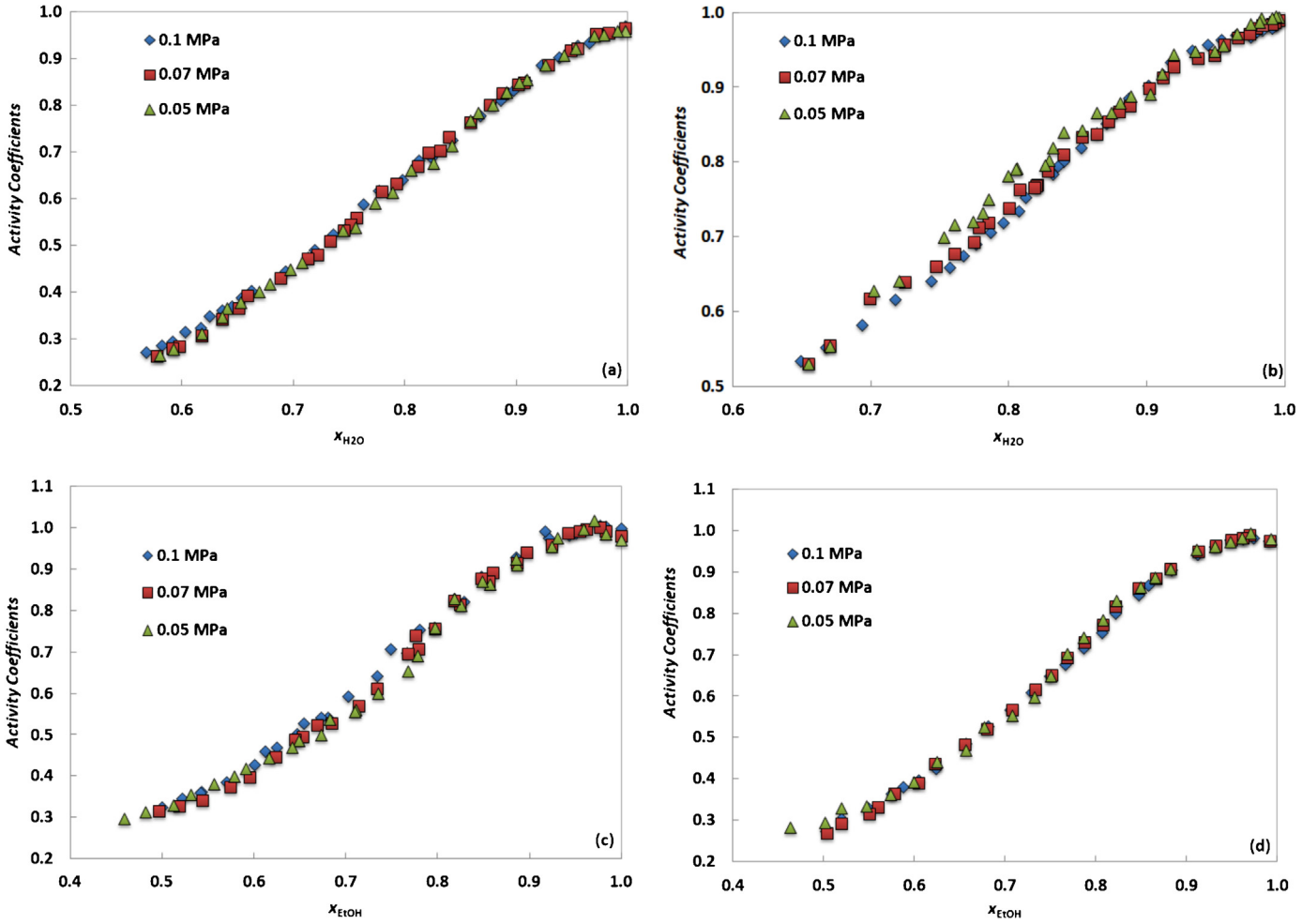

Fig. 7. Activity coefficients for the systems (a) [C_2mim][Cl] + H_2O, (b) [C_6mim][Cl] + H_2O, (c) [C_4mim][Cl] + Ethanol and (d) [C_6mim][Cl] + ethanol.

Table 9
NRTL model binary interaction parameters (J mol^{-1}) for the systems: 1 – water, 2 – ethanol and 3 – ionic liquid. α_{13} = 0.2 and α_{23} = 0.3.

Ionic liquid	Δg_{13}	Δg_{31}	Δg_{23}	Δg_{32}
[C_2mim][Cl]	−1841.6	−11,871	1366.4	−6543.7
[C_4mim][Cl]	−4666.2	−10,222	−5853.7	−6236.2
[C_6mim][Cl]	4318.6	−10,435	−7638.2	−6419.8
[$N_{111(2OH)}$][Cl]	3961.8	−10,718	16,113	−9128.3

Table 10
Average absolute deviations (%AAD) in water (x_{H_2O})/ethanol (x_{EtOH}) mol fractions for the systems studied at 0.1, 0.07 and 0.05 MPa.

Ionic liquid		p (MPa)		
		0.1	0.07	0.05
[C_2mim][Cl]	H_2O	0.887	0.921	1.03
	EtOH	2.77	1.47	1.74
[C_4mim][Cl]	H_2O	0.574	0.464	0.659
	EtOH	0.615	0.961	1.04
[C_6mim][Cl]	H_2O	0.857	0.520	0.844
	EtOH	0.613	0.489	0.878
[$N_{111(2OH)}$][Cl]	H_2O	0.273	0.241	0.426
	EtOH	0.640	0.471	0.473

of the local optima solutions found were recorded and sorted by their quality (decreasing value of ϕ^*).

Table 9 summarizes the best set of values that were found for the NRTL parameters of the systems under study. The values of the residual function ϕ at the optimum varied from 0.1×10^{-2} (water–[$N_{111(2OH)}$][Cl] pair) to 7×10^{-2} (ethanol–[C_2mim][Cl]). The number of local optima found were comprised between 3 (for the pair ethanol–[C_2mim][Cl]) and 42 (ethanol–[$N_{111(2OH)}$][Cl] pair). The solutions delivered by CONOPT corresponded typically to the best local solutions known for each problem. Table 10 lists the average absolute deviation (AAD%) values in the molar fractions x_{H_2O} and x_{EtOH} defined as

$$\%\mathrm{AAD} = \left(\frac{100}{Np}\right) \sum_{i=1}^{Np} \left| x_{\mathrm{calc},i} - x_{\mathrm{exp},i} \right| \quad (10)$$

for each water-IL and ethanol-IL binary systems and pressure datasets. In the T–x binary diagrams for the different ionic liquids in Figs. 1–6, it can be observed that the NRTL model is consistently able to provide a good fit of the experimental data. Nevertheless, it should be noted that the binary parameter values reported here were obtained considering only binary data, and consequently should be used with care in extrapolations to ternary systems and for solvent mole fractions outside the regions where they were correlated.

5. Conclusions

A new microebulliometer for the measurement of the boiling temperatures of ionic liquid systems was developed and validated with success. It allows the measurement of VLE data for solutions of ionic liquids in volatile solvents using small quantities of ionic liquids.

Boiling temperatures for systems of four chloride containing ionic liquids with water and ethanol are reported, with six of these systems reported for the first time in the open literature. The results show that the activity coefficients for these systems are temperature dependent, suggesting that these systems present positive excess enthalpies.

The VLE parameters in the NRTL model for water–IL and ethanol–IL binary pairs for four different ionic liquids were estimated by minimizing a weighted sum of squared residuals of the molar fractions of the solvent (water or ethanol). A good fit of the experimental data was obtained, which makes the NRTL model suitable to support the preliminary design of extractive distillation schemes, considering these ILs as potential entrainers.

Acknowledgments

The authors are thankful for financial support from Fundação para a Ciência e a Tecnologia (Project PTDC/EQU-FTT/102166/2008), Laboratório Associado Centro de Investigação em Materiais Cerâmicos e Compósitos (Project Pest-C/CTM/LA0011/2011), the Doctoral grant (SFRH/BD/64338/2009) of José F.O. Granjo and Post-Doctoral grants (SFRH/BPD/82264/2011 and SFRH/BPD/76850/2011) of Pedro J. Carvalho and Imran Khan, respectively.

References

[1] M. Seiler, D. Kohler, W. Arlt, Sep. Purif. Technol. 29 (2002) 245–263.
[2] Z. Lei, C. Li, B. Chen, Separ. Purif. Rev. 32 (2003) 121–213.
[3] A.B. Pereiro, J.M.M. Araújo, J.M.S.S. Esperança, I.M. Marrucho, L.P.N. Rebelo, J. Chem. Thermodyn. 46 (2012) 2–28.
[4] M. Seiler, C. Jork, A. Kavarnou, W. Arlt, R. Hirsch, AlChE J. 50 (2004) 2439–2454.
[5] N. Calvar, B. González, E. Gómez, Á. Domínguez, J. Chem. Eng. Data 51 (2006) 2178–2181.
[6] J. Zhao, C.C. Dong, C.X. Li, H. Meng, Z.H. Wang, Fluid Phase Equilib. 242 (2006) 147–153.
[7] V.H. Alvarez, S. Mattedi, M. Aznar, J. Chem. Thermodyn. 43 (2011) 895–900.
[8] N.V. Plechkova, K.R. Seddon, Chem. Soc. Rev. 37 (2008) 123–150.
[9] J. Wang, D. Zheng, L. Fan, L. Dong, J. Chem. Eng. Data 55 (2010) 2128–2132.
[10] R. Chen, L. Zhong, C. Xu, J. Chem. Eng. Data 57 (2012) 155–165.
[11] A.E. Andreatta, M. Francisco, E. Rodil, A. Soto, A. Arce, Fluid Phase Equilib. 300 (2011) 162–171.
[12] A. Arce, J. Martínez-Ageitos, A. Soto, Fluid Phase Equilib. 122 (1996) 117–129.
[13] N. Calvar, B.A. González, E. Goĭmez, A.N. Domiĭnguez, J. Chem. Eng. Data 54 (2009) 1004–1008.
[14] N. Calvar, B. González, E. Gómez, A. Domínguez, Fluid Phase Equilib. 259 (2007) 51–56.
[15] L.Z. Zhang, Y. Ge, D.X. Ji, J.B. Ji, J. Chem. Eng. Data 54 (2009) 2322–2329.
[16] H. Renon, J.M. Prausnitz, AlChE J. 14 (1968) 135–144.
[17] J.P. O'Connell, J.M. Haile, Thermodynamics: Fundamentals for Applications, Cambridge University Press, New York, 2005.
[18] R. Kato, M. Krummen, J. Gmehling, Fluid Phase Equilib. 224 (2004) 47–54.
[19] J. Zhao, X.-C. Jiang, C.-X. Li, Z.-H. Wang, Fluid Phase Equilib. 247 (2006) 190–198.
[20] A. Chapeaux, L.D. Simoni, T.S. Ronan, M.A. Stadtherr, J.F. Brennecke, Green Chem. 10 (2008) 1301–1306.
[21] P.J. Linstrom, W.G. Mallard (Eds.), NIST Chemistry WebBook, NIST Standard Reference Database Number 69, National Institute of Standards and Technology, Gaithersburg, MD, 2012 http://www.webbook.nist.gov
[22] DIPPR 801 Thermophysical Property Database and DIADEM Predictive Software, 2000.
[23] A.S. Drud, J. Comput. 6 (1992) 207–216.
[24] O.a.M.S.D. GAMS Corporation, <http://www.gams.com/dd/docs/solvers/oqnlp.pdf>, 2010.